
ASSESSMENT OF UNCERTAINTIES IN THE COMPUTATION OF ATMOSPHERIC CORRECTION PARAMETERS FOR LANDSAT 5 TM AND LANDSAT 7 ETM+ THERMAL BAND FROM ATMOSPHERIC CORRECTION PARAMETER (ATMCORR) CALCULATOR

Barnabas Morakinyo^{1,2,3,4*}, Samantha Lavender^{2,3} and Victor Abbott²

(1) Department of Surveying & Geoinformatics, Faculty of Environmental Sciences, Baze University, Abuja, Nigeria; barnabas.ojo@bazeuniversity.edu.ng

(2) School of Marine Science & Engineering, University of Plymouth, Plymouth, UK

(3) Pixalytics Ltd, 1 Davy Rd, Tamar Science Park, Plymouth, Devon, PL6 8BX, UK

(4) ARGANS Ltd, 1 Davy Rd, Tamar Science Park, Plymouth, Devon, PL6 8BX, UK

ABSTRACT: *This research examines the uncertainties present when computing atmospheric correction parameters (upwelling (L_u) and downwelling (L_d) radiances, and transmittance (τ)) for the 9 flaring sites in Rivers State, Nigeria; and to estimate the total uncertainty introduced into the land surface temperature (LST) when they are applied. 7 Landsat 5 Thematic Mapper (TM) and 7 Landsat 7 Enhanced Thematic Mapper Plus (ETM+) from 04 March 2000 to 08 August 2012 with < 10 % cloud contamination were considered in order to evaluate a trend. All the sites are located within a single Landsat scene (Path 188, Row 057). Option B of the Atmospheric Correction Parameter (ATMCORR) Calculator was adopted to obtain L_u , L_d and τ for Landsat scenes analysed. The L_u , L_d and τ obtained were applied to the calibrated at-sensor radiance band 6 (high gain) data to compute the surface-leaving radiance (L_λ) with the emissivity (ϵ) of each station estimated by using standard values for determined land surface cover. The Planck equation was inverted using the calibration constants to derive LST. To determine the uncertainties introduced by applying the calculated L_u , L_d and τ , an uncertainty analysis was undertaken. The difference between the L_u , L_d and τ interpolated for each study site and that of reference site (Chokocho) were calculated and used for the analysis with 4 L_λ scenarios. The results show that the larger the % of water body at the site, the higher is the uncertainty introduced into LST retrieved from Landsat scene; and that the maximum uncertainty obtained for all sites are below the expected maximum error (0.5 ± 0.8 K). Therefore, it was concluded that ATMCORR Calculator, have the ability to provide an automated method to derive L_u , L_d and τ needed for generating LST in the Niger Delta.*

KEYWORDS: atmospheric correction, atmospheric correction parameters (atmcorr) calculator, emissivity, land surface temperature (lst), Niger Delta.

INTRODUCTION

An atmospheric correction is required to retrieve the real surface parameters by removing the atmospheric effects, such as (potentially) thin clouds (Inamdar et al., 2008); molecular and aerosol scattering, absorption by gases (such as water vapour, ozone, oxygen) and aerosol, and sometime also the correction for cloud shadows, upward emission of the radiation from the Earth surface (Qin et al., 2011); environmental radiance which produces the adjacency effects, variation of

illumination geometry including the Sun's azimuth and zenith angles, and ground slope (Mather, 2004).

Removing the effects of the atmosphere in the thermal region is an essential step when using thermal band imagery for absolute temperature studies, i.e. to make the correction from Top-of-Atmosphere (TOA) radiance or temperature to surface-leaving radiance (L_{λ}) or temperature (Otukei and Blaschke, 2011; Qin et al., 2011; Barsi et al., 2003). The emitted signal from the ground can be both attenuated and enhanced by the atmosphere (Barsi et al., 2005). As the Landsat 5 TM and Landsat 7 ETM+ instruments only have a single thermal band (band 6 with 10.40-12.50 μm wavelength), there is no inherently methodology to correct for atmospheric effects unlike with multiband thermal sensors that utilise the differential absorption in adjacent bands (Qin et al., 2001; Wan and Dozier, 1996). Therefore, ancillary atmospheric data are required.

Various methods have been developed to solve the atmospheric correction process for Thermal Infrared (TIR) data dedicated to single-channel sensors. The available methods can be classified into four categories: The single-channel algorithm, which requires total atmospheric water content values only (Jiménez-Muñoz et al., 2003); the mono-window algorithm, which requires air temperature data only (Qin et al., 2001); the look-up tables approach, which supposes an exhaustive learning database (Jiménez-Muñoz et al., 2009); and the physical approach, which requires the calculation of atmospheric parameters with a radiative transfer model and demands detailed knowledge of the atmospheric profile (Coll et al., 2010; Barsi et al., 2003).

The gaps before this research is that in the Niger Delta, limited research into removal of atmospheric effects on thermal band of satellites data (Landsat 5 Thematic Mapper (TM) and Landsat 7 Enhanced Thematic Mapper Plus (ETM+)) has been published to date, and no studies applied atmospheric correction parameters (ATMCORR) Calculator tool methodology for derivation of atmospheric correction parameters (upwelling (L_u), downwelling (L_d) and transmittance (τ)) for Landsat 5 TM and Landsat 7 ETM+. Therefore, the two basic research questions for this study are: (1) How accurately can the ATMCORR Calculator derive the atmospheric correction parameters (upwelling (L_u), downwelling (L_d) and transmittance (τ)) for Landsat 5 TM and Landsat 7 ETM+ thermal band in the Niger Delta region? (2). What is the maximum expected uncertainty range introduced into LST(s) generated from using the derived L_u , L_d and τ obtained from the ATMCORR Calculator? Based on these questions, the primary aim of this research was to evaluate the uncertainties present when computing L_u , L_d and τ for the 9 flaring sites in Rivers State of the Niger Delta (Nigeria). In addition, to estimate the total uncertainty introduced into the LST when they are applied. The specific objectives set to answer the above research questions are: (1). Derivation of L_u , L_d and τ from the ATMCORR Calculator; (2). Retrieval of Land Surface Temperature (LST) from Landsat 5 TM and Landsat 7 ETM+ using the derived L_u , L_d and τ from the ATMCORR Calculator; (3). Determination of the amount of uncertainties introduced into LST by applying the calculated L_u , L_d and τ .

MATERIALS AND METHODS

This study focuses on 9 oil and gas facilities located in the Rivers State of the Niger Delta region, Nigeria. The selection of these flare sites was based on the function of the facility e.g. refineries, liquefied natural gas (LNG) plant, flow stations, terminals, oil wells. Those chosen include: Eleme Refinery I and II Petroleum Companies; Bonny LNG plant; Onne, Rukpokwu, Umurolu, Obigbo, and Chokocho Flow Stations; and Elem Kalabari oil well (Figure 1). Each site was investigated as a 12 by 12 km area. Table 2 shows the geographic coordinates for each site.



Figure 1: Gas flaring site locations in Rivers State, Nigeria; Source: Google Earth, 2019; Ite et al., 2013.

Data used

The U.S. Geological Survey (USGS) data archive was systematically searched for scenes with < 10 % cloud contamination. All the sites are located within a single Landsat scene (Path 188, Row 057), with the results of the search being 7 Landsat 5 TM and 7 Landsat 7 ETM+ scenes from 04 March 2000 to 08 August 2012 (Table 1). The scenes were downloaded from the USGS Earth Resources Observation and Science (EROS) Data Centre website (<http://earthexplorer.usgs.gov/>) using the Glovis/Earth Explorer interfaces. The processing level for all the scenes is L1T, which means systematic radiometric correction, and geometric correction using both ground control points (GCPs) and a digital elevation model were applied (Morakinyo, 2015).

Table 1: Date and time of the Landsat 5 TM & Landsat 7 ETM+ scenes used

Scene Identity No.	Date	UTC Time (hh:mm)
LT51880572000064SGS00	04 March 2000	09:37
LT51880572000336AGS00	01 December 2000	09:35
LT51880572002037SGS00	06 February 2002	09:34
LT51880572002325SGS00	21 November 2002	09:33
LT51880572004043ASN01	12 February 2004	09:34
LT51880572004331ASN00	26 November 2004	09:34
LT51880572006016ASN00	16 January 2006	09:35
LE71880572006352ASN00	18 December 2006	09:35
LE71880572008006ASN00	06 January 2008	09:35
LE71880572008326ASN00	21 November 2008	09:34
LE71880572010043ASN00	12 February 2010	09:37
LE71880572010347ASN00	13 December 2010	09:38
LE71880572012017ASN01	17 January 2012	09:39
LE71880572012225ASN00	12 August 2012	09:40

Atmospheric Correction Parameter (ATMCORR) Calculator

To obtain the atmospheric correction parameters (L_u , L_d and τ) for Landsat 5 TM and Landsat 7 ETM+, the Atmospheric Correction Parameter (ATMCORR) Calculator that was developed by Barsi et al. (2003) and made available to the public at <http://atmcorr.gsfc.nasa.gov> (Coll et al., 2010) was employed. However, according to Barsi et al. (2005), the limitations of the ATMCORR Calculator are as follows: (1) ATMCORR Calculator generates parameters for a single point. This may be sufficient to describe the atmosphere across a whole Landsat scene in some cases, but where there is a considerable elevation change, more than one run of the Calculator may become necessary. (2) There is no automatic check for clouds or discontinuities in the interpolated atmosphere. Therefore, the profiles contained in the emailed summary file need to be checked for problems. (3) National Center for Environmental Prediction (NCEP) data in the format currently used is not available for the entire Landsat 5 TM and Landsat 7 ETM+. The NCEP holdings include all dates since 01 March 2000. (4) The interpolation in time and space is linear, which may not be the most appropriate method for sampling weather fronts or areas with significant diurnal heating cycle. (5) The emissivity (ϵ) of the target must be known in order to calculate land surface temperature (LST). In addition, the initial validation of ATMCORR Calculator by Barsi et al. (2005) showed a systematic error of > 1.5 K; and a bias of 0.5 ± 0.8 K for LSTs generated after correction.

Operational principle of ATMCORR Calculator

The ATMCORR Calculator is a single-channel method that applies the MODerate-Resolution Atmospheric Radiance and Transmittance (MODTRAN) algorithm to allow a user to accurately retrieve LST from Landsat thermal data (Barsi et al., 2003). It uses NCEP to provide atmospheric data for 28 altitudes; NCEP has global coverage, but a coarse 1° by 1° grid (spatial resolution) and 6 hour time step (temporal resolution) (Figure 2 A). Currently, ATMCORR Calculator only provides atmospheric correction parameters for dates from 01 March 2000 as this is when that dataset began (McCarville et al, 2011).

The Calculator requires a specific date, time and location as the input (Table 2), and has 2 methods for resampling the grid to the specific site: “Use atmospheric profile for closest integer lat/long” or “Use interpolated atmospheric profile for given lat/long”. The first extracts the grid corner that is closest to the input location for the 2 temporal samples bounding the input time, and interpolates to the given time. The second option extracts the profiles for the 4 grid corners surrounding the location before and after the time input. The corner profiles are interpolated for each time, and then the resulting time profiles are interpolated resulting in a single profile (Barsi et al., 2003).

The local surface conditions supplied by the user will be used, and the lower layers of the atmosphere will be interpolated from 3 km above sea level to the surface to remove any discontinuities. Another option is the choice between a summer and winter standard atmosphere for the upper layer (Barsi et al., 2005). In addition, the user can select the TM bandpass, the ETM+ bandpass, or no spectral bandpass, in which case; only the interpolated atmospheric profiles for use in a radiative transfer model are output (Barsi et al., 2014; Barsi et al., 2003). The resulting integrated L_u , L_d , and τ and all the atmospheric data used to generate the results are output to the browser and emailed to the user.

For this research, the coordinate of each flare station (latitude (ϕ) and longitude (λ)), year, month, date and time of data acquisition (hours and minutes) was inputted into the calculator. Option B, which is to use an interpolated atmospheric profile for the given (ϕ) and (λ), was chosen alongside the mid-latitude summer standard atmosphere. Landsat 5 band 6 and Landsat 7 band 6 spectral response curves were chosen for the Landsat 5 TM data, and Landsat 7 ETM+ data. In less than 4 minutes, the data supplied were processed and the result displayed on the computer screen and within a supplied e-mail address (Figure 2B). Figure 2A shows the locations of the 9 investigated flare sites in (ϕ) and (λ) (See Figure 1 and Table 2 for the numbering).

The L_u , L_d , and τ were applied to the calibrated at-sensor radiance band 6 (high gain) data to compute the surface-leaving radiance (L_s) (Equation 1). For this research, the 4 land cover (LC) types (vegetation, soil, built up and water) with their % identified at these sites during ground validation (02 July to 04 August 2012 and 04 February to 05 March 2019) was derived using MATLAB code with cluster analysis. The LC types was clarified using images held within Google Earth and Digital Global (<http://browse.digitalglobe.com/imagefinder/public.do>) such as WorldView-1 and 2, IKONOS pseudo-true colour images; and Landsat imagery (bands 1-4 and 6), and Red Green Blue (RGB) pseudo-true colour composite images. The method used to estimate ϵ value for LC types at these sites is based on the ϵ of 4 LC types present at each site. Each pixel LC types were considered for the entire site and their ϵ values (both minimum (min) and maximum (max)) were taken from the literature. Mean of ϵ value for LC types for each single pixel obtained from using their (min) and (max) values from the literature were calculated. Average of ϵ (min) and ϵ (max) results were obtained for each pixel and the same procedure was repeated for all pixels in the selected 12 by 12 km area (Morakinyo, 2015).

Table 2: Input data for the computation of Thermal Atmospheric Parameters by the Calculator

S/N	Flare station	Latitude (ϕ)	Longitude (λ)	Acquired date (yr mm dd)	Acquired time (hr:mm:ss)
1.	Eleme Refinery I	4.728772	7.118861	2000/03/04	09:35:36
2.	Eleme Refinery II	4.762175	7.111025	2002/02/06	09:33:30
3.	Onne Flow station	4.712321	7.141187	2004/02/12	09:35:33
4.	Bonny LNG	4.414188	7.139889	2006/01/16	09:41:21
5.	Rukpokwu Flow Station	4.930011	7.016102	2008/01/06	09:35:26
6.	Umurolu Flow Station	4.829012	7.109021	2008/11/21	09:34:31
7.	Obigbo Flow Station	4.892001	7.120012	2010/02/12	09:37:36
8.	Elem Kalabari oil well	4.554221	6.978213	2010/12/13	09:38:30
9.	Chokocho Flow Station (a reference site)	5.007669	7.019187	2012/01/17	09:35:35

Table 3: Emissivity values picked from the Look Up Table (LUT)

Land cover types at the 9 sites investigated	ϵ Min.	ϵ Max.	Reference
Short grass	0.979	0.983	Labeled and Stoll, 1991
Bushes (≈ 100 cm)	0.960	0.994	Labeled and Stoll, 1991
Densely vegetated areas		0.980	Jin and Liang, 2006
Bare soil.		0.960	Humes et al., 1994
Sandy soil		0.930	Hipps, 1989
Loamy soil		0.914	van de Griend et al., 1991
Water body.	0.950	0.980	Masuda et al., 1988
		0.990	Stathopoulou and Cartalis, 2007
Medium built up area		0.964	Stathopoulou and Cartalis, 2007
Densely built-up urban		0.946	Stathopoulou and Cartalis, 2007

Therefore, the ϵ value for each Landsat pixel is a combination of the ϵ value of background features except of any flare present within the pixel. The authors adopted an independent method of using LC types at each site for the correction of ϵ value rather than Global Land Cover (GLC) data from USGS in order to ensure quality control primarily (Table 3).

$$L_{\lambda} = ((L_s - L_u) / \epsilon \tau) - ((1 - \epsilon) / \epsilon) \times L_d \quad (\text{Wm}^{-2}\text{sr}^{-1}\mu\text{m}^{-1}) \quad (1)$$

Where,

L_s = Radiometrically corrected Landsat thermal band 6 radiance (high gain);

L_u = Upwelling radiance;

L_d = Downwelling radiance;

τ = Atmospheric transmission;

ϵ = emissivity.

L_u , L_d , and τ are atmospheric correction parameters for the Landsat thermal band.

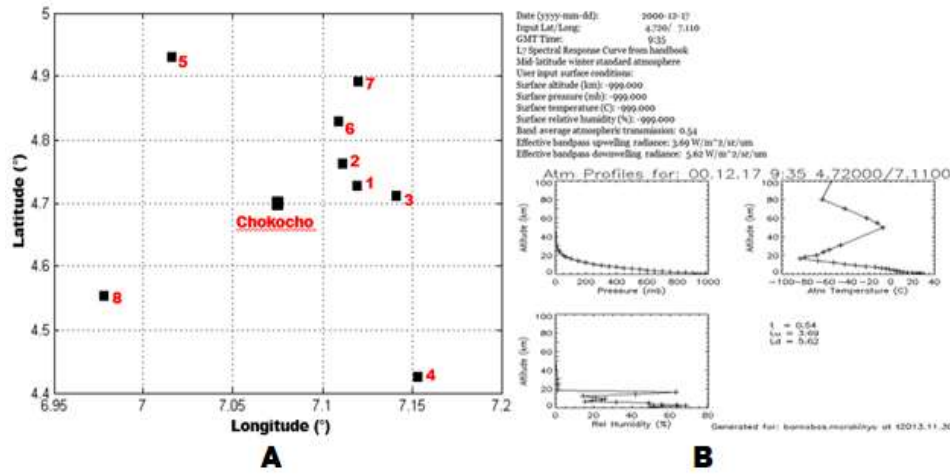


Figure 2: (A) Latitude and Longitude of the 9 flare sites in Rivers State, Nigeria; (B) Atmospheric Correction Parameters and its Profile from the ATMCORR Calculator.

Then, the Planck equation was inverted using the calibration constants to derive LST (Equation 2).

$$LST = \frac{K_2}{\ln((K_1/L_i) + 1)} \quad (2)$$

Where, K_1 and K_2 are thermal band calibration constants calculated for the Landsat sensor characteristics. For Landsat 5 TM, $K_1 = 607.76$ ($Wm^{-2}sr^{-1}\mu m^{-1}$) and $K_2 = 1260.56$ (K); for Landsat 7 ETM+, $K_1 = 666.09$ ($W m^{-2} sr^{-1}\mu m^{-1}$) and $K_2 = 1282.71$ (K).

Assessment of uncertainties

In order to determine the uncertainties introduced by applying the calculated L_u , L_d and τ an uncertainty analysis was undertaken. The difference between the L_u , L_d and τ interpolated for each study site and those of Chokocho site were calculated and used for this analysis. 4 different L_i scenarios were examined using equation 1, and are represented by equations 3 to 6.

$$L_{\lambda 1} = (L_s - (L_{uc} + \Delta L_u)) / (\varepsilon \times \tau_c) - (1 - \varepsilon) / (\varepsilon) \times L_{dc} \quad (Wm^{-2}sr^{-1}\mu m^{-1}) \quad (3)$$

$$L_{\lambda 2} = (L_s - L_{uc}) / (\varepsilon \times \tau_c) - (1 - \varepsilon) / (\varepsilon) \times (L_{dc} + \Delta L_d) \quad (Wm^{-2}sr^{-1}\mu m^{-1}) \quad (4)$$

$$L_{\lambda 3} = (L_s - L_{uc}) / (\varepsilon \times (\tau_c + \Delta \tau)) - (1 - \varepsilon) / (\varepsilon) \times L_d \quad (Wm^{-2}sr^{-1}\mu m^{-1}) \quad (5)$$

$$L_{\lambda 4} = (L_s - L_{uc}) / (\varepsilon + \Delta \varepsilon) \times (\tau_c) - (1 - \varepsilon) / (\varepsilon) \times L_{dc} \quad (Wm^{-2}sr^{-1}\mu m^{-1}) \quad (6)$$

Where,

L_s = Radiometrically corrected Landsat thermal band 6 radiance (high gain);

L_{uc} = Upwelling radiance for Chokocho Flow Station site;

L_{dc} = Downwelling radiance for Chokocho Flow Station site;

τ_c = Transmittance for Chokocho Flow Station site; ε = emissivity;

ΔL_u = Difference between the L_u for Chokocho Flow Station site and other sites;

ΔL_d = Difference between the L_d for Chokocho Flow Station site and other sites;

$\Delta \tau$ = Difference between the τ for Chokocho Flow Station and other sites;

$\Delta \varepsilon$ = Difference between the ε for Chokocho Flow Station and other sites.

The computed L_λ obtained for equations 3 to 6 for each site were used to compute LST for each site, based on equation 2.

RESULTS

The minimum and maximum value from the difference between the L_u , L_d , τ and ε for the Chokocho site and for each site is presented in Table 4. In Table 5, the minimum and maximum value of combine uncertainty introduced into LST; the minimum and maximum value of LSTs retrieved; and the % of water body for each site are presented. Figure 3 shows the plot of the retrieved LSTs for each site for the period undertaken.

Table 4: Minimum and maximum values of ΔL_u , ΔL_d , $\Delta \tau$, and $\Delta \varepsilon$

S/N	Flaring site	ΔL_u (min.)	ΔL_u (max.)	ΔL_d (min.)	ΔL_d (max.)	$\Delta \tau$ (min.)	$\Delta \tau$ (max.)	$\Delta \varepsilon$ (min.)	$\Delta \varepsilon$ (max.)
1	Eleme I	0.00	0.80	0.01	1.31	0.00	0.13	0.002	0.029
2	Eleme II	0.00	0.97	0.00	1.34	0.00	0.13	0.007	0.053
3	Onne	0.01	1.02	0.01	1.38	0.00	0.13	0.001	0.043
4	Bonny LNG	0.03	1.16	0.03	1.65	0.00	0.17	0.014	0.034
5	Rukpokwu	0.01	0.72	0.01	1.07	0.00	0.07	0.000	0.032
6	Umurolu	0.01	0.71	0.01	1.06	0.00	0.07	0.000	0.032
7	Obigbo	0.00	0.66	0.01	1.11	0.00	0.08	0.004	0.027
8	Elem	0.01	0.74	0.00	1.47	0.00	0.07	0.001	0.032

Table 5: Minimum and maximum values of combine uncertainty introduced into LST, minimum and maximum value of LST retrieved and the % of water body for each site.

S/N	Flaring site	Minimum error (%)	Minimum error (K)	Maximum error (%)	Maximum error (K)	Minimum LST (K)	Maximum LST (K)	% of water body
1	Eleme I	0.00367	3.67×10^{-3}	17.148	0.172	286.046	320.415	50
2	Eleme II	0.00729	7.29×10^{-3}	17.462	0.175	284.731	315.127	53
3	Onne	0.00195	1.95×10^{-3}	16.863	0.169	282.992	317.130	48
4	Bonny LNG	0.00293	2.93×10^{-3}	28.523	0.285	274.491	313.612	90
5	Rukpokwu	0.00170	1.70×10^{-3}	13.660	0.137	282.486	323.702	34
6	Umurolu	0.00210	2.10×10^{-3}	15.540	0.155	283.471	314.741	40
7	Obigbo	0.00210	2.10×10^{-3}	13.430	0.134	285.010	324.162	31
8	Elem	0.00150	1.50×10^{-3}	19.240	0.192	278.629	312.843	65

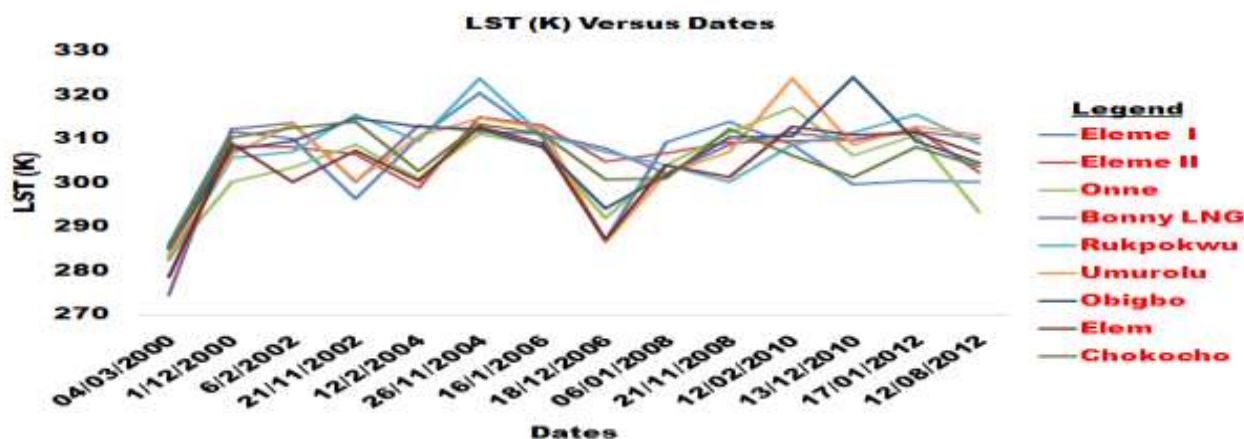


Figure 3: The retrieved LSTs for flaring sites in Rivers State, Nigeria.

DISCUSSION

Generally, the results in Table 5 shows that the larger the % of water body at the site, the higher is the uncertainty introduced into LST retrieved from Landsat scene. In addition, Barsi et al. (2005) stated that the expected maximum uncertainty range when atmospheric parameters from ATMCORR Calculator are applied is ± 0.8 K for LSTs generated. The maximum uncertainty obtained for all the 9 sites are far below 0.8 K. One of further researches that could be carried out on this study in order to enhance further analysis is to repeat the same for a place like Iraq or Saudi Arabia (dry desert environment) since Nigeria is in humid tropical environment.

CONCLUSION

Based on the results of maximum uncertainty introduced into LSTs in Table 5 and its comparison with that of Barsi et al. (2005), it can be concluded that ATMCORR Calculator, have the ability to provide an automated method to derive atmospheric correction parameters needed for generating LST in the Niger Delta region.

Acknowledgements

This work was supported by the Tertiary Education Trust Fund (TETFund) of Nigeria, under Academic Staff Training and Development (AST&D) Scholarship. Thanks to USGS for the provision of Landsat data and MODTRAN ATMCORR Calculator; and also to Jill Schwarz for guidance and MATLAB coding.

References

- Barsi, J. A. (2014). Personal communication: "A Solution that Latitude and Longitude with more than one decimal place should not be inputted into the Calculator". Landsat Project Science Office, Science Systems and Applications, Inc. Greenbelt, United States of America.
- Barsi, J. A., Schott, J. R., Palluconi, F. D, and Hook, S. J. (2005). "Validation of a Web-Based Atmospheric Correction Tool for Single Thermal Band Instruments". Earth

- Observing Systems X, Proceedings of SPIE 5882: 0277-786X/05/\$15· doi: 10.1117/12.619990
- Barsi, J. A., Barker, J. L, and Schott, J. R. (2003). "An Atmospheric Correction Parameter Calculator for a Single Thermal Band Earth-Sensing Instrument". International Geoscience Remote Sensing Symposium 5: 3014-3016.
- Coll, C., Galve, J. M., Sanchez, J. M, and Caselles, V. (2010). "Validation of Landsat 7ETM+ Thermal-Band Calibration and Atmospheric Correction with Ground-Based Measurement". IEEE Transaction on Geoscience and Remote Sensing 48(1): 547-555.
- Hipps, L. E. (1989). "The Infrared Emissivities of Soil and Artemisia Tridentate and Subsequent Temperature Corrections in a Shrub-steppe Ecosystem". Remote Sensing of Environment 27: 337-342.
- Humes, K. S., Kustas., W. P., Moran, M. S., Nichols, W. D. and Wertz, M. A. (1994). "Variability of Emissivity and Surface Temperature Over a Sparsely Vegetated Surface". Water Resources Research 30(5): 1299-1310.
- Inamdar, A. K., French, A., Hook, S., Vanghan, G. and Lueckett, W. (2008). "Land surface temperature retrieval at high spatial and temporal resolutions over the south-western United States". Journal of Geophysical Research: Atmospheres 113 (D7) 1-18.
- Jin, M and Liang, S. (2006). "An Improved Land Surface Emissivity Parameter for Land Surface Models Using Global Remote Sensing Observations". Journal of Climate 19: 2867-2881.
- Jiménez-Muñoz, J. C. and Sobrino, J. A. (2003). "A Generalized Single-Channel Method for Retrieving Land Surface Temperature from Remote Sensing Data". Journal of Geophysical Research, 108, doi:10.1029/2003JD003480.
- Jiménez-Muñoz, J. C., Cristóbal, J., Sobrino, J. A., Soria, G., Ninyerola, M. and Pons, X. (2009). "Revision of the Single-Channel Algorithm for Land Surface Temperature Retrieval From Landsat Thermal-Infrared Data". IEEE Transaction on Geoscience and Remote Sensing 47(1): 339-349.
- Labeled, J and Stoll, M. P. (1991). "Spatial Variability of Land Surface Emissivity in the Thermal Infrared Band: Spectral Signature and Effective Surface Temperature". Remote Sensing of Environment 38(1-7).
- Masuda, K., Takashima, T and Y, Takayama. (1988). "Emissivity of Pure and Sea Waters for the Model Sea Surface in the Infrared Window Regions". Remote Sensing of Environment 24:313-329.
- Mather, P. M. (2004). "Computer processing of remotely sensed images: An Introduction", 3rd Edition. West Sussex, England, John Willey and Sons.
- McCarville, D., Buenemann, M., Bleiweiss, M. and Barsi, J. A. (2011). "Atmospheric Correction of Landsat Thermal Infrared Data: A Calculator Based on North America Regional Reanalysis (NARR)". ASPRS Annual Conference, Milwaukee, Wisconsin: 12.
- Morakinyo, B. O. (2015). "Flaring and Pollution Detection in the Niger Delta Using Remote Sensing". PhD Thesis, School of Marine Science and Engineering, University of Plymouth, Plymouth, UK.
- Otukei, J. R. and Blaschke, T. (2011). "You Know The Temperature at a Weather Station But Do You Know It Anywhere Else? Assessing the Land Surface Temperature Using Landsat ETM+ Data". Proceedings of The first Conference on Advances in Geomatics Research:

169-179.

- Qin, Z., Olmo, G. D. and Karnieli, A. (2001). "Derivation of Split Window Algorithm and Its Sensitivity Analysis For Retrieving Land Surface Temperature From NOAA-Advanced Very High Resolution Radiometer Data". *Geophysical Research*: 22655-22670.
- Qin, Z. H., Karnieli, A. and Berliner, P. (2001). "A Mono-Window Algorithm for Retrieving Land Surface Temperature from Landsat TM Data and Its Application to the Israel-Egypt Border Region. *International Journal of Remote Sensing* 22: 3719-3746.
- Qin, Q., Zhang, N., Nan, P. and Chai, L. (2011). "Geothermal Area Detection Using Landsat ETM+ Thermal Infrared Data and Its Mechanistic Analysis: A case study in Tengchong, China". *International Journal of Applied Earth Observation and GeoInformation* 13: 552-559.
- Stathopoulou, M and Cartalis, C. (2007). "Daytime Urban Heat Island from Landsat ETM+ and Corine Land Cover Data: An Application to Major Cities in Greece". *Solar Energy* 81: 358-368.
- van de Griend, A. A., Owe, M., Groen, M. and Stoll, M. P. (1991). "Measurement and Spatial Variation of Thermal Infrared Surface Emissivity in a Savannah Environment". *Water Resources Research* 27: 371-379.
- Wan, Z. and Dozier, J. (1996). "A Generalized Split-Window Algorithm for Retrieving Land Surface Temperature Measurement from Space". *IEEE Transactions on Geoscience and Remote Sensing* 34: 892-905.